YALE JOURNAL OF BIOLOGY AND MEDICINE 92 (2019), pp.413-422.

ORIGINAL CONTRIBUTION

YALE JOURNAL OF BIOLOGY AND MEDICINE
YJBM
CELEBRATING 90 YEARS 1928–2018

Identifying Specific Subcellular Organelle Damage by Photosensitized Oxidations

Tayana Mazin Tsubone[a,b], Waleska Kerllen Martins[a,c], and Maurício S. Baptista[a,*]

[a]*Department of Biochemistry, Institute of Chemistry, University of Sao Paulo, Brazil;* [b]*Institute of Physics, University of Sao Paulo, Brazil;* [c]*Anhanguera University of Sao Paulo, Brazil*

The search for conditions that maximize the outcome of Photodynamic Therapy (PDT†) continues. Recent data indicate that PDT-induced cell death depends more on the specific intracellular location of the photosensitizer (PS) than on any other parameter. Indeed, knowledge of the PS intracellular location allows the establishment of clear relationships between the mechanism of cell death and the PDT efficacy. In order to determine the intracellular localization sites of a given PS, classical co-localization protocols, which are based in the comparison of the emissive profiles of organelle-specific probes to those of the PS, are usually performed. Since PSs are usually not efficient fluorophores, co-localization protocols require relatively high PS concentrations (micromolar range), distorting the whole proposal of the experiment, as high PS concentration means accumulation in many low-affinity sites. To overcome this difficulty, herein we describe a method that identifies PS intracellular localization by recognizing and quantifying the photodamage at intracellular organelles. We propose that irradiation protocols and characterization of major sites of photodamage results from many cycles of photosensitized oxidations, furnishing an integrated picture of the PS location. By comparing the results of protocols based in either method, we showed that the analysis of the damaged organelles can be conducted at optimal conditions (low PS concentrations), providing clear correlations with cell death mechanisms, which is not the case for the results obtained with co-localization protocols. Experiments using PSs that target either mitochondria or lysosomes were described and investigated in detail, showing that evaluating organelle damage is as simple as performing co-localization protocols.

INTRODUCTION

Photosensitization reactions play fundamental roles on the interaction between light and matter. The basic concepts of these reactions have been applied to the medical field in a procedure known as Photodynamic Therapy (PDT), which is being used to treat a variety of diseases such as malignant tumors [1-5] and many non-oncological diseases such as age-related macular degeneration [6], psoriasis [7], arthritis [8,9], and photoinactivation of vi-

*To whom all correspondence should be addressed: Mauricio S. Baptista, Department of Biochemistry, Institute of Chemistry, University of Sao Paulo, SP, Brazil, Tel: +55 (11)-3091-8952, Email: baptista@iq.usp.br.

†Abbreviations: PS, photosensitizer; PDT, Photodynamic Therapy; PBS, phosphate buffer saline; FBS, fetal bovine serum; IC_{50}, half of maximal inhibitory concentration; CisDiMPyP, meso-cis-di(N-methyl-4-pyridyl) diphenyl porphyrin dichloride; $TPPS_{2a}$, meso-tetraphenylporphine disulphonic acid dihydrochloride (adjacent isomer); DMMB, 1,9-dimethyl methylene blue; LED, light emission diode; DAPI, 4,6-diamidino-2-phenylindole; Rh123, rhodamine; JC-1, 5,5′,6,6′-tetrachloro-1,1′,3,3′-tetrethyl benzimidazolylcarbocyanine iodide.

Keywords: Photodamage, photosensitizer, organelles, specificity, intracellular localization, Photodynamic Therapy

Author Contributions: T.M.T. and W.K.M. designed, performed experiments, and analyzed the data. M.S.B coordinated the work and reviewed the manuscript. All authors contributed to writing the manuscript.

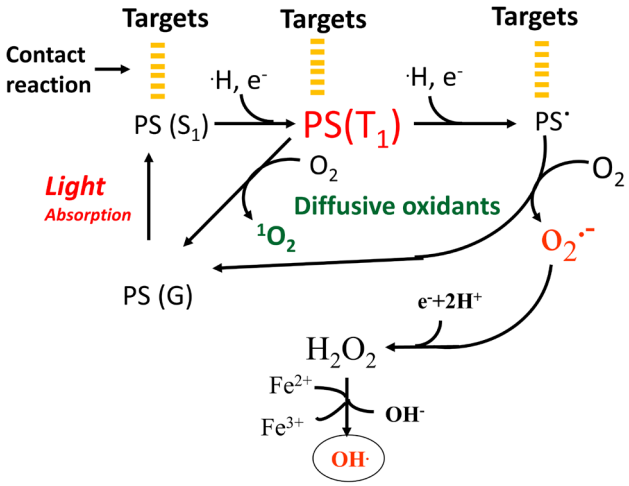

Figure 1. Mechanism of photosensitization. The photosensitizer (PS) absorbs light forming an excited singlet state ($PS(S_1)$). The $PS(S_1)$ is converted to triplet excited state ($PS(T_1)$) via the intersystem crossing. Then, $PS(T_1)$ can transfer energy to oxygen, generating singlet oxygen ($^1O_2$) or abstraction of electron or hydrogen-producing radicals such as $O_2^{\bullet-}$ and $OH^{\bullet}$.

rus and bacteria [10]. The photodynamic effect starts with the light absorption by the photosensitizer (PS), initially forming singlet ($^1PS^*$) and subsequently (as a result of intersystem crossing) triplet excited states ($^3PS^*$). $^3PS^*$ are both stronger reducing and oxidizing agents than the ground state molecule (PS) and have a longer lifetime than the singlet excited state ($^1PS^*$). Consequently, $^3PS^*$ can transfer energy to oxygen (type II process) forming singlet oxygen ($^1O_2$) or can directly react with biological substrates (type I process) [11,12].

In most cases, $^1O_2$ is the main oxidant species that triggers the harmful effects of PDT by damaging many biomolecules (guanine in nucleic acids, tryptophan, tyrosine, histidine, methionine in proteins, unsaturated lipids). The lifetime of $^1O_2$ in living cells have been reported to be very short, ~0.4 μs, meaning that $^1O_2$ diffusion distance is limited to ~ 0.3 μm. A likely contribution of highly reactive hydroxyl radical ($OH^{\bullet}$) is expected. Hydroxyl radical ($OH^{\bullet}$), which is the most reactive oxygen radical known, is produced by the Fenton reaction with the reduction of hydrogen peroxide. Its diffusive pathway has not been measured ($OH^{\bullet}$ is too reactive), but undoubtedly it is very small. There are also the direct-contact reactions that damage targets at molecular contacts with the PS, generating many reactive radicals [11-13]. Hydrogen peroxide and anion radical superoxide ($O_2^{\bullet-}$) can also be generated during the photosensitized process. These species have low reactivity and can diffuse for dozen of micrometers [13,14]. They can induce biological responses at distances, but these effects are secondary to the photon absorption and photosensitization processes that will damage targets in the close proximity of the PS [14,15] (Figure 1).

Even though several parameters such as lower tendency of PS aggregation, higher absorption in the red spectral region and higher efficiency in the generation of $^1O_2$ [16-20] are important parameters for the optimization of the PDT efficiency, recent reports demonstrated that the intracellular PS localization site and the consequent type of cell death mechanism are more relevant for the final photodynamic efficiency [21,22]. Indeed, several authors have shown that subcellular localization is a fundamental factor to be considered in terms of controlling PDT efficacy, since it defines the type of organelle damage, and consequently the type of cell death mechanism [22-25]. Hence, defining the PDT intracellular target is essential [26-30]. Confocal fluorescence microscopy has provided the possibility to evaluate the subcellular localization of PSs by co-localization protocols, in which cells are co-stained with probes, which specifically accumulate in certain organelles and PSs. By integrating the cellular regions whose fluorescence profile of both the probe and the PS co-stain, the areas of PS localization is estimated [23,31,32]. Although being conceptually simple the protocols present limitations.

There are conceptual and practical limitations of the classical co-localization protocols that should be explained. The conceptual one is that the exact site of photodamage is difficult to define, since diffusive species do play a secondary role in the biological response. However, this is not terribly important since the primary relevant species are very reactive and have a limited pathway in cells (described above). The major limitation is a practical one. Classical co-localization protocols rely on probes with high fluorescence quantum yields, but usually this is not the case for most PSs, since they are designed to generate triplet species. Therefore, usually the co-local-

ization protocols require high PS concentrations to compensate the low fluorescence emission. Consequently, the key intrinsic intracellular targets may be blurred because PSs will also localize in many low-affinity binding sites. Interestingly, by using methods that sense the biological activity/structure of intracellular organelles, we can perform the organelle-targeting analysis at very low PS concentration. In here, we describe a protocol to identify intracellular sites of photodamage after irradiating cells previously incubated with nanomolar PS concentrations and subsequently treated with probes that sense organelle damage. By using this protocol, we could establish good correlations between the major sites of intracellular damage mediated PSs and their photobiological effects.

PROTOCOL

Preparation of Cells in Microscopy Coverslips

1. Wash glass coverslips with 70% (v/v) ethanol for cleaning and sterilization.

2. Remove the excess of ethanol by washing with MilliQ water and expose coverslips under UVC light for 15 minutes.

3. Put the clean, sterile, and dried coverslip into each well of the plate.

4. Choose adherent mammalian cells, such as HeLa cells (human cervical adenocarcinoma) [33], to perform intracellular organelle-targeting for photodamage.

NOTE: We used HeLa cells (ATCC® CCL-2) here as a biological cell model.

5. Seed ≈2-3 x 10^5 cells on each 6-well plate containing the coverslip previously cleaned and sterilized.

NOTE: Depending on the cell type, a surface coating to facilitate the adhesion of cells to the glass coverslip is required. The source and concentration of coating agent may vary depending on the histological cell type. Of note, HeLa cells can adhere directly on the glass in presence of medium supplemented with 10% (v/v) fetal bovine serum (FBS) without previous coating.

6. Incubate the seeded cells in a 37°C incubator under a moist atmosphere of 5% carbon dioxide for 18 h to 24 h to reach at least a cellular confluence of 75%.

NOTE: Culture conditions and incubation time to reach an optimal cell density depends on the cell type and the population doubling times.

Photosensitization of Cells

1. After having selected a suitable incubation time for reaching optimal confluence, wash the cells with phosphate buffer saline (PBS) and incubate with photosensitizer of interest in DMEM media containing 1% (v/v) FBS during 3 hours in a 37°C incubator under a moist atmosphere of 5% carbon dioxide.

NOTE: The photosensitizer concentration and time incubation should be set according to the half-maximal inhibitory concentration (IC_{50}) values previously obtained. For instance, the photosensitizers used were $TPPS_{2a}$ and CisDiMPyP in a level at nanomolar range (*i.e.,* 30 nM and 100 nM), respectively.

CAUTION: The photosensitizer solubility in aqueous media depends on its physical-chemical molecular properties. Optimal conditions of media to solubilize photosensitizer need to be previously determined.

2. After a suitable incubation time with photosensitizer, wash the cells with PBS before the photosensitization step that is performed using light emission diode (LED) at a determined irradiance and time. Use light dose of ≈2 J/cm^2 with LED with maximum wavelength in 522 ± 20 nm as an optimal condition to perform photosensitization in HeLa cells using 30 nM $TPPS_{2a}$ and 100 nM CisDiMPyP.

NOTE: Dark control is performed under similar conditions than described above. However, in dark control, the cells are incubated with a photosensitizer, but without light irradiation.

NOTE: The maximum wavelength of LED and optimal conditions of irradiations may differ regarding the system used. It should be previously determined in agreement with the photosensitizer type.

3. Once the irradiation is completed, the PBS media is replaced by DMEM 10% (v/v) FBS and the cells are incubated in a 37°C incubator under a moist atmosphere of 5% carbon dioxide, during the required time to evaluate the photodamaged organelle after PDT (named here as "*post-PDT time*").

Staining Intracellular Targets with Specific Organelle Probes After Photosensitization

1. 3 h after photosensitization, incubate the cells using a particular probe for mitochondria or lysosomes. Stain the HeLa organelles using 1 μM mitochondrial probe or 200 nM lysosomal probe for 30 minutes in a 37°C incubator under a moist atmosphere of 5% carbon dioxide.

NOTE: Other organelles can be selected for investigation in terms of intracellular photodamage, *e.g.*, endoplasmic reticulum. The following conditions probe concentration or incubation time depends on the probe source and histological cell type used in the experiment.

2. Wash cells with PBS twice and fix them in 4% (w/v) formaldehyde in PBS pH 7.4 for 15 minutes at room temperature in the absence of light.

NOTE: It is highly recommended to perform the manipulation with formaldehyde by using protective glasses and gloves.

3. Wash cells with PBS three times at 5-minute intervals at room temperature and in the absence of light.

Table 1. Excitation and emission wavelengths of confocal microscopy selected according to the probes.

Probe	$\lambda_{excitation}$	$\lambda_{emission}$	Setup Microscope
Mitochondrial probe	579 nm	599 nm	Laser for excitation in 543 nm and filter set emission in 565 to 615 nm
Lysosomal probe	577 nm	590 nm	Laser for excitation in 543 nm and filter set emission in 565 to 615 nm

4. Remove any excess of liquid from the sample and add one drop of the antifade reagent containing 4,6-diamidino-2-phenylindole (DAPI) onto a clean slide and carefully lower the coverslip onto the antifade reagent to avoid trapping any air bubbles.

5. Seal it with nail polish and store the sample protected from light at 4˚C until the analyses under confocal microscopy.

NOTE: Sealing the edges retards the oxidation and extends the life of the sample for several months at 4˚C.

Confocal Microscopy

1. Check the excitation and emission wavelengths available at confocal microscopy required for the chosen probe. The lasers and filters considering the mitochondrial and lysosomal probes are listed in Table 1.

Quantifying the Microscopy Data by Using Image J

1. Open the image of interest on Image J software.

2. Select the cell to be analyzed by delimiting a square around (Figure 2).

3. Select the red channels to quantify the pixels only from red fluorescence (Figure 3).

4. In "*Analyze*" and "*Set Measurements*," select "*Mean gray values*" and "*Integrated density*" (Figure 4). "*Mean gray values*" represents the sum of the gray values of all the pixels in the selection divided by the number of total pixels. "*Integrated density*" the product of Area and Mean Gray Value.

5. Go back to the image of interest and in "*Analyze*"→ "*Measure*" (Figure 5) to get the mean gray values and integrated density of red pixels at the selected square area.

6. Perform it to every single cell from different images of independent experiments and normalized the number of fluorescent pixels in the cells treated by control cells and expressed as arbitrary units (a. u.).

REPRESENTATIVE RESULTS

The mechanism of dye accumulation in lysosomes is based in the positive electrochemical potential kept in the internal lumen of this organelle. Weak base compounds, which freely diffuse through membranes in their unprotonated form, become protonated and consequently trapped in the acidic environment of lysosomes. The term "lysosomotropic agents" is commonly used to define weak amine bases that retain 100-fold higher concentrations within lysosomes compared to the cytosol [34-36]. The lysosomal probe used here consists of a fluorophore linked to a weak base. Therefore, in case of damaged lysosomes the staining fails. As can be observed in Figure 6, lysosomes are well stained in both non-treated and cells treated with PS that are not concentrated in lysosomes, *e.g.*, CisDiMPyP. However, after irradiating cells previously incubated with a PS that accumulates in lysosomes, *e.g.*, $TPPS_{2a}$ [21,37,38], lysosome staining becomes vanishingly small (non-visible at the conditions used in this study) (Figure 6).

A similar concept can be extrapolated to other organelles. For example, mitochondria exhibit a negative transmembrane potential of around -180 mV due to ion proton pumps of the respiratory electron transport chain [39]. Consequently, mitochondria attract positively charged dyes by electrostatic forces [40,41]. The mitochondrial probe used here contains a reduced positive group derivative of dihydro-X-rosamine that leads to mitochondrial membrane accumulation. However, it does not emit fluorescence unless it is oxidized. Therefore, it becomes fluorescent only when accumulated in mitochondria that is actively breathing [42,43]. Note that red fluorescence is only present in non-treated cells or in cells treated with photosensitizer that does not accumulate in mitochondria, *e.g.*, $TPPS_{2a}$ (Figure 7). On the other hand, cells treated with a photosensitizer that is known to photodamage mitochondria, *e.g.*, CisDiMPyP [21], are not stained by this mitochondrial probe (Figure 7).

The principle of this methodology has been used in different works from our and other groups. For instance, our recent work showed that irradiating cells previously incubated with DMMB (1,9-dimethyl methylene blue) at nanomolar levels reduce staining of both mitochondria and lysosome probes, consequently implying the parallel damage in both mitochondria and lysosome [22]. Another example, reported by Xu *et al*. [44], demonstrated that the red fluorescence of JC-1 (5,5′,6,6′-tetrachloro-1,1′,3,3′-tetrethyl benzimidazolylcarbocyanine iodide) gradually and proportionally decreases according to the higher level of mitochondrial damage in HeLa cells after photosen-

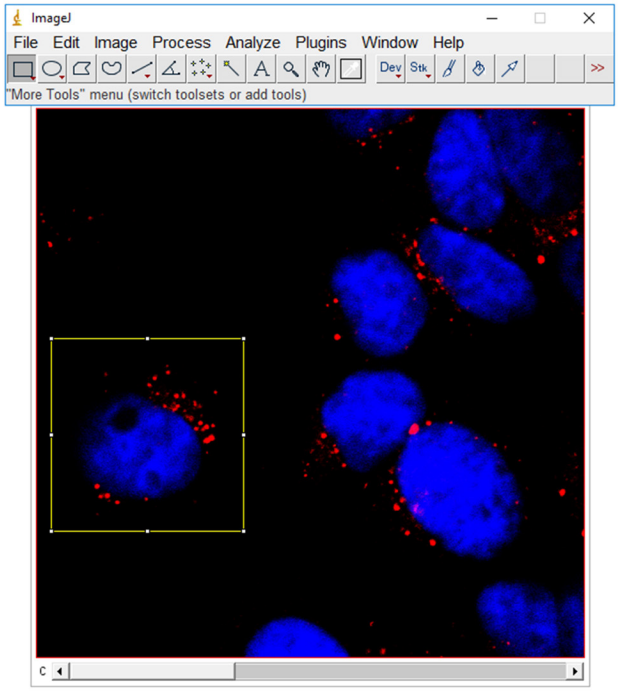

Figure 2. Representative image to show the selected cell in the yellow rectangle. Blue color represents the fluorescence of DAPI and red color the fluorescence of lysosomal probe.

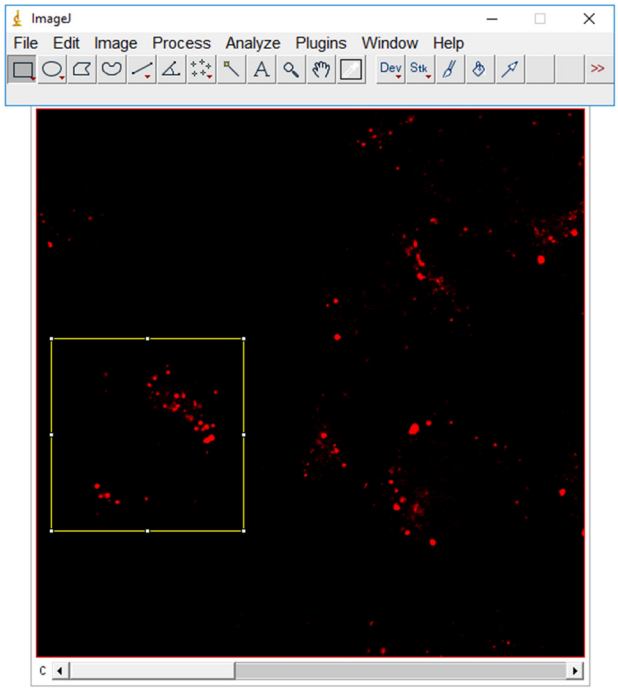

Figure 3. Representative image of only the red channel evident to quantify the pixels. Yellow rectangle depicts the analyzed cell and red color the fluorescence of lysosomal probe.

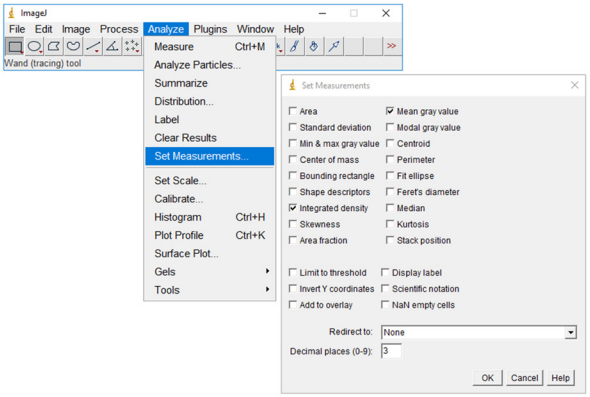

Figure 4. Steps to measure the red pixels.

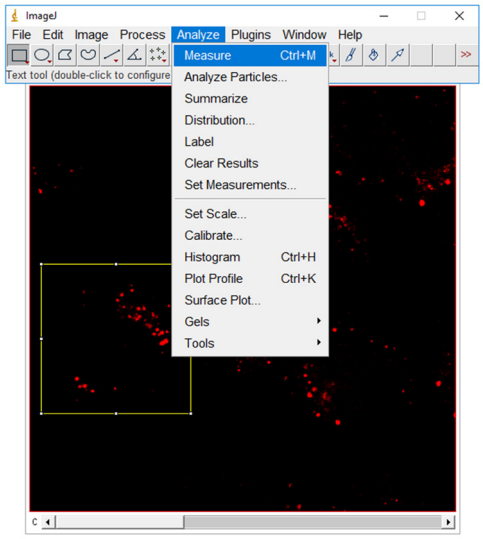

Figure 5. Finally measuring it and getting the values.

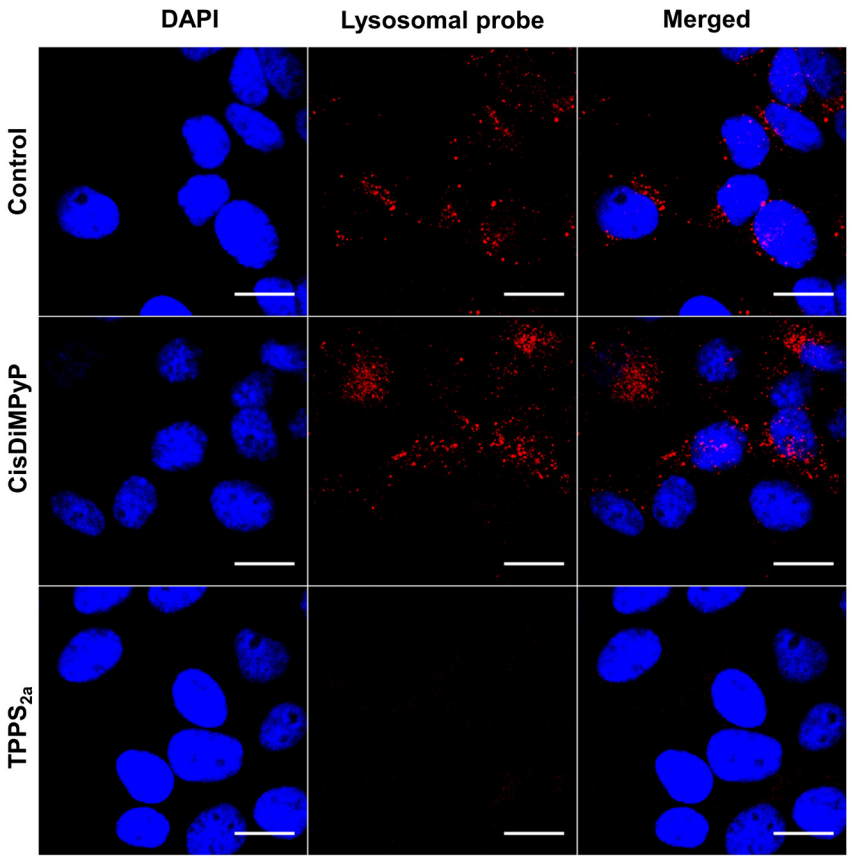

Figure 6. Fluorescence images 3 hours after PDT-treatment of HeLa cells with 100 nM CisDiMPyP and 30 nM $TPPS_{2a}$ and non-treated cells (Control). First column: blue fluorescence of DAPI-stained nuclei; second column: red fluorescence of lysosomes; third column: both channels (blue and red) merged. Scale bar represents 20 μm. This figure was reproduced from Tsubone *et al*. [21], with permission from Springer Nature under the terms of the Creative Commons Attribution 4.0 International License.

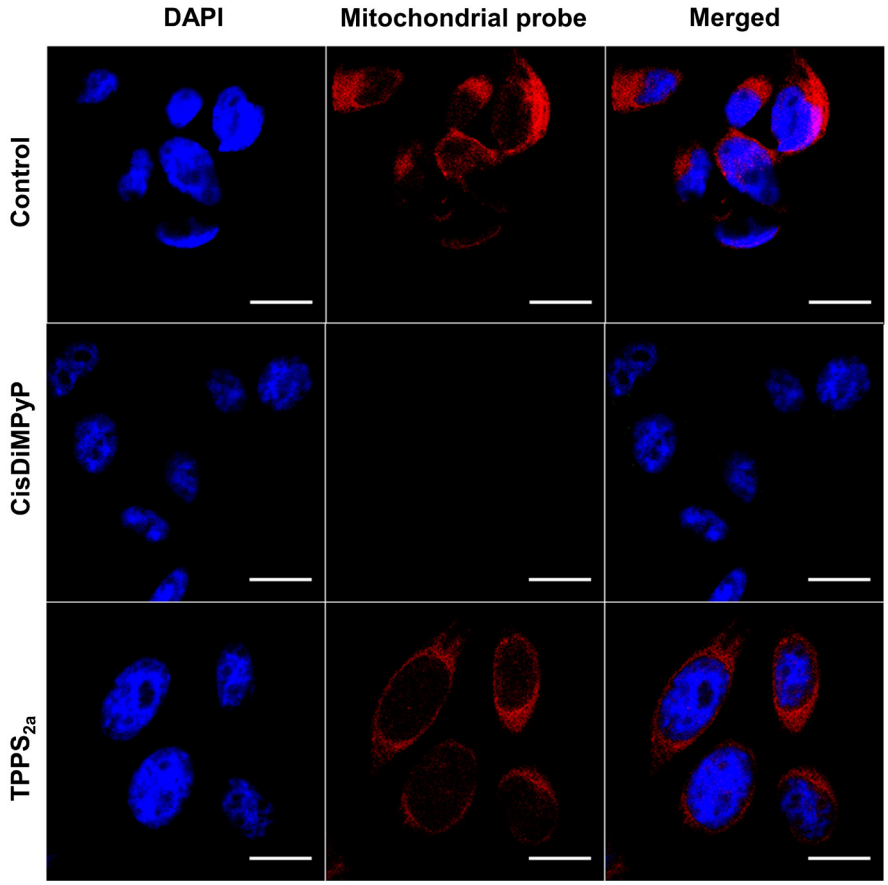

Figure 7. Fluorescence images 3 hours after PDT-treatment of HeLa cells with 100 nM CisDiMPyP and 30 nM $TPPS_{2a}$ and non-treated cells (Control). First column: blue fluorescence of DAPI-stained nuclei; second column: red fluorescence of mitochondria; third column: both channels (blue and red) merged. Scale bar represents 20 μm. This figure was reproduced from Tsubone *et al*. [21], with permission from Springer Nature under the terms of the Creative Commons Attribution 4.0 International License.

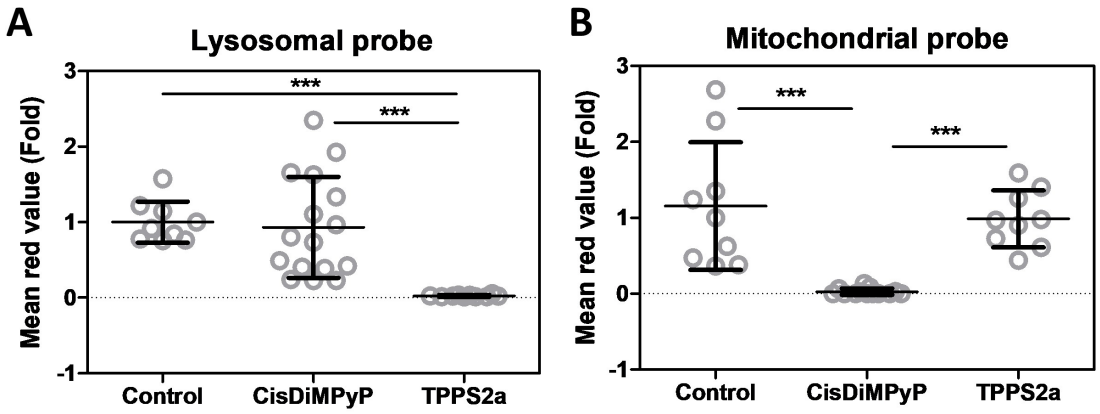

Figure 8. Average of red fluorescence calculated by relative to the fluorescent pixels number in the treated cells compared to control (taken as 100%). (**A**) Lysosomal probe and (**B**) Mitochondrial probe. Each circle represents one cell, and lines indicate the mean ± SD. *p<0.05, **p<0.03 and ***p<0.001 are considered statistically significant.

Table 2. Co-localization percentage of porphyrins with mitochondrial probe and lysosomal probe after 3 h incubation in HeLa cells. This figure was reproduced from Tsubone *et al*. [21], with permission from Springer Nature under the terms of the Creative Commons Attribution 4.0 International License.

Overlay (PS/organelle)	Lysosomal probe (L)	Mitochondrial probe (M)
CisDiMPyP	20% ± 2%	38% ± 5%
$TPPS_{2a}$	39% ± 4%	30% ± 5%

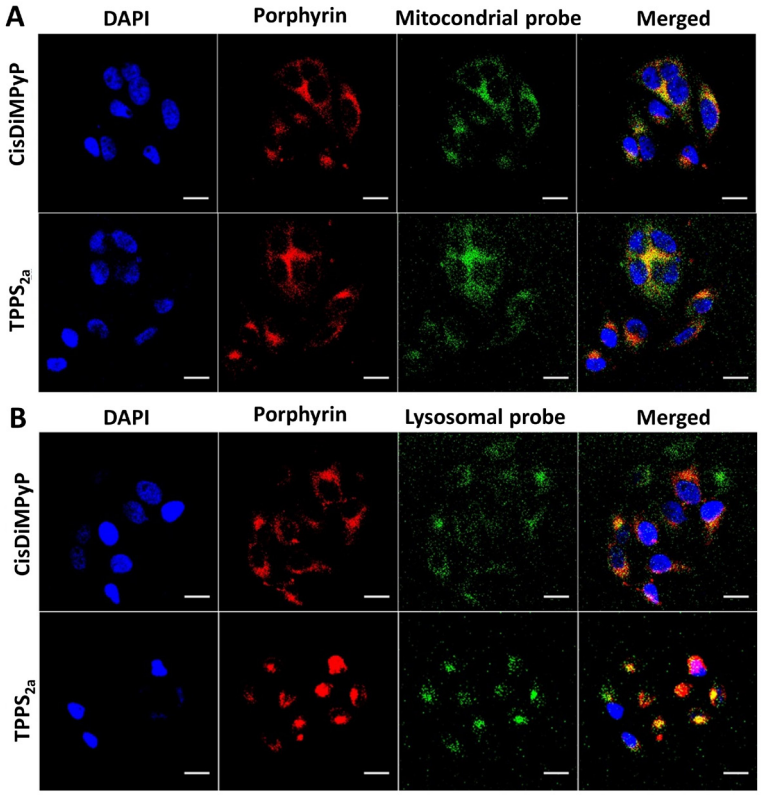

Figure 9. (**A**) Confocal fluorescence microscopy images of HeLa cells, showing blue fluorescence for DAPI-stained nuclei, red fluorescence related to photosensitizer (1 μM) and green fluorescence related to mitochondria (150 nM of the probe). The right column shows the overlay from three channels (blue, red and green). (**B**) Confocal fluorescence microscopy images of HeLa cells with blue fluorescence of nucleus (DAPI), red fluorescence of porphyrins (1 μM) and green fluorescence of lysosomes (150 nM of probe). The right column shows the overlay from three channels (blue, red and green). Scale bars correspond to 20 μm. This figure was reproduced from Tsubone *et al*. [21], with permission from Springer Nature under the terms of the Creative Commons Attribution 4.0 International License.

sitization with a cationic porphyrin derivative (mitoTPP).

This methodology allows not only the visualization of photodamaged organelles, but also the estimate of mean fluorescence values in terms of pixels before and after the treatment (Figure 8). Details about how to quantify the number of fluorescent pixels is described in protocol item 5.

DISCUSSION

Identification of the intracellular targets of photodamage is an essential tool in terms of controlling and maximizing the PDT efficiency [21-23,25]. The classical experimental protocol used to define the subcellular localization sites relies on the treating cells with both the PS and an organelle marker before light exposition [24,31,37,45-48]. Calculating the number of pixels that show fluorescence of both PS and marker provides the percentage of the PS accumulation within the specific organelle. This classical methodology usually requires the incubation of cells with relatively high PS concentrations, suffering from accuracy and precision.

To exemplify the limitations of co-localization assays, Figure 9 illustrates data from HeLa cells co-stained with PSs (1 μM) and probes (Table 2). Overlay values suggests partial localization of both CisDiMPyP and TPPS2a at lysosomes and mitochondria (Table 2). Of note, CisDiMPyP and TPPS2a at low concentrations, specifically accumulate within mitochondria and lysosomes, respectively (Table 2). This information is key to define the respective mechanisms of cell death which are apoptosis and autophagy related cell death for CisDiMPyP and TPPS2a, respectively [21,33,34].

Acknowledgments: This work was supported by FAPESP scholarship (2013/16532-1) and FAPESP research grant (2013/07937-8).

REFERENCES

1. Spring BQ, Rizvi I, Xu N, Hasan T. The role of photodynamic therapy in overcoming cancer drug resistance. Photochem Photobiol Sci. 2015;14(8):1476–91.
2. Allison RR, Sibata CH, Downie GH, Cuenca RE. A clinical review of PDT for cutaneous malignancies. Photodiagn Photodyn Ther. 2006;3(4):214–26.
3. Hasan T, Ortel B, Moor AC, Pogue BW. Photodynamic therapy of cancer. In: Radiation Oncology. 1988. p. 43–55.
4. Usuda J, Kato H, Okunaka T, Furukawa K, Yamada K, Suga Y, et al. Photodynamic Therapy (PDT) for Lung Cancers. J Thorac Oncol. 2006;1(5):489–93.
5. Babilas P, Schreml S, Landthaler M, Szeimies RM. Photodynamic therapy in dermatology: state-of-the-art. Photodermatol Photoimmunol Photomed. 2010;26(3):118–32.
6. Bressler NM, Bressler SB. Photodynamic Therapy with Verteporfin (Visudyne): Impact on Ophthalmology and Visual Sciences. Invest Ophthalmol Vis Sci. 2000;41(3):624–8.
7. Morton CA, Morton CA, Brown SB, Brown SB, Collins S, Collins S, et al. Guidelines for topical photodynamic therapy: report of a workshop of the British Photodermatology Group. Br J Dermatol. 2002;146(4):552–67.
8. Trauner KB, Gandour-Edwards R, Bamberg M, Shortkroff S, Sledge C, Hasan T. Photodynamic synovectomy using benzoporphyrin derivative in an antigen-induced arthritis model for rheumatoid arthritis. Photochem Photobiol. 1998;67(1):133–9.
9. Trauner KB, Hasan T. Photodynamic Treatment of Rheumatoid and inflammatory Arthritis. Photochem Photobiol. 1996;64(5):740–50.
10. Jori G, Brown SB. Photosensitized inactivation of microorganisms. Photochem Photobiol Sci. 2004;3(5):403–5.
11. Itri R, Junqueira HC, Mertins O, Baptista MS. Membrane changes under oxidative stress: the impact of oxidized lipids. Biophys Rev. 2014;6(1):47–61.
12. Bacellar I, Oliveira MC, Dantas L, Costa E, Junqueira HC, Martins WK, et al. Photosensitized Membrane Permeabilization Requires Contact-Dependent Reactions between Photosensitizer and Lipids. J Am Chem Soc. 2018;140:9606–15.
13. Gutowski M, Kowalczyk S. A study of free radical chemistry: their role and pathophysiological significance. Acta Biochim Pol. 2013;60(1):1–16.
14. Baptista MS, Cadet J, Di Mascio P, Ghogare AA, Greer A, Hamblin MR, et al. Type I and Type II Photosensitized Oxidation Reactions: Guidelines and Mechanistic Pathways. Photochem Photobiol. 2017;93(4):912–9.
15. Bacellar IO, Tsubone TM, Pavani C, Baptista MS. Photodynamic Efficiency: From Molecular Photochemistry to Cell Death. Int J Mol Sci. 2015;16:20523–59.
16. Tsubone TM, Braga G, Vilsinski BH, Gerola AP, Hioka N, Caetano W. Aggregation of Aluminum Phthalocyanine Hydroxide in Water/Ethanol Mixtures. J Braz Chem Soc. 2014;25(5):890–7.
17. Bonnett R. Photosensitizers of the porphyrin and phthalocyanine series for Photodynamic Therapy. Chem Soc Rev. 1995;24:19–33.
18. Pushpan SK, Venkatraman S, Anand VG, Sankar J, Parmeswaran D, Ganesan S, et al. Porphyrins in photodynamic therapy - a search for ideal photosensitizers. Curr Med Chem Anticancer Agents. 2002;2:187–207.
19. Derosa MC, Crutchley RJ. Photosensitized singlet oxygen and its applications. Coord Chem Rev. 2002;233–234:351–71.
20. Uchoa AF, De Oliveira KT, Baptista MS, Bortoluzzi AJ, Iamamoto Y, Serra OA. Chlorin photosensitizers sterically designed to prevent self-aggregation. J Org Chem. 2011;76(21):8824–32.
21. Tsubone TM, Martins WK, Pavani C, Junqueira HC, Itri R, Baptista MS. Enhanced efficiency of cell death by lysosome-specific photodamage. Sci Rep. 2017;7(1):6734.
22. Martins WK, Santos NF, Rocha C S, Bacellar IO, Tsubone TM, Viotto AC, et al. Parallel damage in mitochondria and lysosomes is an efficient way to photoinduce cell death. Autophagy. 2019;15(2):259–79.
23. Castano AP, Demidova TN, Hamblin MR. Mechanisms in photodynamic therapy: part one - Photosensitizers, photochemistry and cellular localization. Photodiagn Photodyn Ther. 2004;2004(1):279–93.
24. Oliveira CS, Turchiello R, Kowaltowski AJ, Indig GL, Baptista MS. Major determinants of photoinduced cell death: subcellular localization versus photosensitization efficiency. Free Radic Biol Med. 2011;51(4):824–33.
25. Verma S, Watt GM, Mai Z, Hasan T. Strategies for enhanced photodynamic therapy effects. Photochem Photobiol. 2007;83(5):996–1005.
26. Schlothauer J, Hackbarth S, Röder B. A new benchmark for time-resolved detection of singlet oxygen luminescence - Revealing the evolution of lifetime in living cells with low dose illumination. Laser Phys Lett. 2009;6(3):216–21.
27. Redmond RW, Kochevar IE. Spatially Resolved Cellular Responses to Singlet Oxygen. Photochem Photobiol. 2006;82:1178–86.
28. Hackbarth S, Schlothauer J, Preub A, Roder B. New insights to primary photodynamic effects - Singlet oxygen kinetics in living cells. J Photochem Photobiol B. 2010;98(3):173–9.
29. Bacellar IO, Cordeiro RM, Mahling P, Baptista MS, Röder B, Hackbarth S. Oxygen distribution in the fluid/gel phases of lipid membranes. Biochim Biophys Acta Biomembr. 2019;1861(4):879–86.

30. Dos Santos AF, De Almeida DR, Terra LF, Baptista MS, Labriola L. Photodynamic therapy in cancer treatment - an update review. J Cancer Metastasis Treat. 2019;5(25):1–20.
31. Teiten MH, Bezdetnaya L, Morlière P, Santus R, Guillemin F. Endoplasmic reticulum and Golgi apparatus are the preferential sites of Foscan localisation in cultured tumour cells. Br J Cancer. 2003;88(1):146–52.
32. Wilson BC, Olivo M, Singh G. Subcellular Localization of Photofrin® and Aminolevulinic Acid and Photodynamic Cross-Resistance in Vitro in Radiation-Induced Fibrosarcoma Cells Sensitive or Resistant to Photofrin-Mediated Photodynamic Therapy. Photochem Photobiol. 1997;65(1):166–76.
33. Evans VJ, Earle WR, Sanford KK, Shannon JE, Waltz HK. The preparation and handling of replicate tissue cultures for quantitative studies. J Natl Cancer Inst. 1951;11(5):907–27.
34. Boya P, Kroemer G. Lysosomal membrane permeabilization in cell death. Oncogene. 2008;27:6434–51.
35. Raben N, Shea L, Hill V, Plotz P. Monitoring Autophagy in Lysosomal Storage Disorders. Methods Enzymol. 2009;453(08):417–49.
36. Zong D, Zielinska-Chomej K, Juntti T, Mörk B, Lewensohn R, Hååg P, et al. Harnessing the lysosome-dependent antitumor activity of phenothiazines in human small cell lung cancer. Cell Death Dis. 2014;5:e1111.
37. Berg K, Moan J. Lysosomes as photochemical targets. Int J Cancer. 1994;59(6):814–22.
38. Berg K, Western A, Bommer JC, Moan J. Intracellular localization of sulfonated meso-tetraphenylporphines in a human carcinoma cell line. Photochem Photobiol. 1990;52(3):481–7.
39. Hoye AT, Davoren JE, Wipf P, Fink MP, Kagan VE. Targeting mitochondria. Acc Chem Res. 2008;41(1):87–97.
40. Dessolin J, Schuler M, Quinart A, De Giorgi F, Ghosez L, Ichas F. Selective targeting of synthetic antioxidants to mitochondria: towards a mitochondrial medicine for neurodegenerative diseases? Eur J Pharmacol. 2002;447(2–3):155–61.
41. Lemasters JJ, Ramshesh VK. Imaging of Mitochondrial Polarization and Depolarization with Cationic Fluorophores. Methods Cell Biol. 2007;80(06):283–95.
42. Paxinou E, Weisse M, Chen Q, Souza JM, Hertkorn C, Selak M, et al. Dynamic regulation of metabolism and respiration by endogenously produced nitric oxide protects against oxidative stress. Proc Natl Acad Sci USA. 2001;98(20):11575–80.
43. Ellerby HM, Wadih A, Ellerby LM, Kain R, Kain R, Andrusiak R, et al. Anti-cancer activity of targeted pro-apoptotic peptides. Nat Med. 1999;5(9):1032–8.
44. Xu J, Zeng F, Wu H, Hu C, Wu S. Enhanced Photodynamic E ffi ciency Achieved via a Dual-Targeted Strategy Based on Photosensitizer /Micelle Structure. Biomacromolecules. 2014;15:4249–59.
45. Reiners JJ, Caruso JA, Mathieu P, Chelladurai B, Yin XM, Kessel D. Release of cytochrome c and activation of procaspase-9 following lysosomal photodamage involves Bid cleavage. Cell Death Differ. 2002;9(9):934–44.
46. Pavani C, Uchoa AF, Oliveira CS, Iamamoto Y, Baptista MS. Effect of zinc insertion and hydrophobicity on the membrane interactions and PDT activity of porphyrin photosensitizers. Photochem Photobiol Sci. 2009;8:233–40.
47. Wang JT, Berg K, Høgset A, Bown SG, MacRobert AJ. Photophysical and photobiological properties of a sulfonated chlorin photosensitiser TPCS2a for photochemical internalisation (PCI). Photochem Photobiol Sci. 2013;12:519–26.
48. Woodburn KW, Vardaxis NJ, Hill JS, Kaye AH, Reiss JA, Phillips DR. Evaluation of Porphyrin Characteristics Required for Photodynamic Therapy. Photochem Photobiol. 1992;55(5):697–704.